



of  $\text{SiO}_2$  or  $\text{SiO}_2$  on Si is of particular interest. If one knows the probabilities for various inelastic processes as a function of electron energy, this information can be incorporated in Monte Carlo programs to examine the details of the energy deposition process as discussed earlier for Si [3]. For example, one could study the dependence on layer thickness, the role of interface effects, or the statistics of the energy-loss processes. The more limited purpose of this paper is to describe a model for determining the required probabilities for inelastic events. The model is tested by computing quantities that can be compared with experimental data. In particular we calculate the mean energy loss per unit path length and inelastic mean free path for electrons in  $\text{SiO}_2$  and the mean excitation energy of  $\text{SiO}_2$ .

#### THEORETICAL MODEL

For incident electron energies considered here ( $\leq 10$  keV), the main source of energy loss is due to interactions with the electrons in the medium. The response of a medium to a given energy transfer,  $\omega$ , and momentum transfer  $q$  may be described by a complex dielectric function  $\epsilon(q, \omega)$ . In general,  $\epsilon$  may be a tensor which depends on the direction of  $q$ . In this work it is assumed that the medium is homogeneous and isotropic so that  $\epsilon$  is a scalar quantity which depends on the magnitude of  $q$  and not its direction. If  $\epsilon$  is known, for an electron of kinetic energy  $E$  and velocity  $v$ , the probability of an energy loss  $\omega$  per unit energy loss per unit distance traveled can be determined from [4,5]

$$\tau(E, \omega) = \frac{2}{\pi v^2} \int_{q_-}^{q_+} \frac{dq}{q} \text{Im} [-1/\epsilon(q, \omega)] . \quad (1)$$

The equations in this paper are in Hartree atomic units where  $\hbar = m = e = 1$ . To account for the small relativistic correction at the higher electron energies considered here, the limits on the integral in Eq. (1) are given by

$$q_{\pm} \equiv [2E(1+E/2c^2)]^{\frac{1}{2}} \pm [2E(1+E/2c^2) - 2\omega(1+E/c^2) + \omega^2/c^2]^{\frac{1}{2}}$$

and  $v^2/2 = E(1+E/2c^2)/(1+E/c^2)^2$  with  $c = 137$ . For most of the energy region considered here, these expressions reduce to the usual non-relativistic forms  $E = v^2/2$  and  $q_{\pm} = \sqrt{2}[\sqrt{E} \pm \sqrt{E-\omega}]$ . The quantity  $\tau(E,\omega)$  is also called the differential inverse mean free path, since by integrating it over allowed energy transfers, the inelastic inverse mean path for an electron of energy  $E$  is obtained. In addition, the quantity  $\omega\tau(E,\omega)$  integrated over allowed values of  $\omega$  gives the energy loss per unit path length or, neglecting radiation by the electron, the stopping power of the medium for an electron of energy  $E$ .

The main task then is to find a suitable expression for  $\epsilon(q,\omega) \equiv \epsilon_1(q,\omega) + i\epsilon_2(q,\omega)$  to describe the dielectric response of  $\text{SiO}_2$ . For the purpose of modeling, the electrons in the medium are divided into two groups: valence electrons and inner-shell electrons. A model insulator theory [6] is used to describe the valence electrons, while generalized oscillator strengths are used to describe inner-shell ionization. The theoretical model for  $\epsilon$  is based, in part, on optical data and has been employed previously for other solids [7] as well as for  $\text{SiO}_2$  [8]. The results of Ref. 8 have been improved by doing a more detailed fit of  $\epsilon_2(0,\omega)$ , the imaginary part of the dielectric function for zero momentum transfer, to experimental values [9] of  $\epsilon_2$  for crystalline  $\text{SiO}_2$  of density

2.65 g/cm<sup>3</sup>. The new fit is shown in Fig. 1 by the dashed curve, using a band gap of 8.9 eV [10]. The sharp peak at 10.3 eV is generally agreed to be due to an exciton transition, while the structure at higher energies is less certain and is described by some workers as due to interband transitions [11] or, most recently, as being due to excitonic resonances [10]. The assignment of the processes responsible for these features in  $\epsilon_2$  may be important in examining the detailed energy deposition processes in SiO<sub>2</sub> as was done earlier for silicon [3] and water [12]. The fitting process and the sum-rule checks for overall consistency have been discussed in detail elsewhere [13]. The insulator model describes the dielectric response of 16.8 effective valence electrons per SiO<sub>2</sub> molecule at zero momentum transfer. The effective number of valence electrons decreases to 16 for large momentum transfers as the effective number of inner-shell electrons increases to a value corresponding to the occupation numbers for the inner shells [13].

Given  $\epsilon_2(q,\omega)$  for the valence electrons,  $\epsilon_1(q,\omega)$  was determined from a Kramers-Kronig relation. The total energy-loss function for the medium is given by

$$\text{Im} [-1/\epsilon(q,\omega)] = \text{Im} [-1/\epsilon(q,\omega)]_{\text{val}} + \sum_i \frac{2\pi^2 n_i}{\omega} \frac{df_i(q)}{d\omega} \quad (2)$$

where the first term on the right is the valence electron term as determined by the insulator model and the second term is due to ionization of the inner shells. The generalized oscillator strength for shell  $i$ ,  $df_i(q)/d\omega$ , was taken from McGuire's tables [14] for the K shell of oxygen, from Manson's values [15] for the L shell of silicon, and derived from hydrogenic wave functions [16] for the K shell of silicon. The number of shells

of type  $i$  per unit volume is  $n_i$ . The energy-loss function in Eq. (2) was constructed so that the energy-loss sum rule

$$\int_0^{\infty} d\omega \omega \operatorname{Im} [-1/\epsilon(q,\omega)] = 2\pi^2 n_0 N \quad (3)$$

is obeyed for any  $q$  where  $N = 30$  electrons per  $\text{SiO}_2$  molecule and  $n_0 = 3.930 \times 10^{-3}$  molecules per unit volume in atomic units. The energy-loss function in the  $q = 0$  limit (dashed curve) is shown in Fig. 2 for comparison with that determined by Buechner from electron energy-loss measurements (solid curve) [17]. The main peak in our result lies  $\sim 1$  eV higher than Buechner's, possibly due to a slightly different density. The structure below the main peak is sharper for the insulator model (or the optical data) than in the solid curve.

As a further check on the model dielectric function in the optical limit ( $q = 0$ ), we have evaluated the mean excitation energy  $I$  of crystalline  $\text{SiO}_2$  from [18]

$$\ln I \equiv \frac{1}{2\pi^2 n_0 N} \int_0^{\infty} d\omega \omega \operatorname{Im} [-1/\epsilon(0,\omega)] \ln \omega \quad (4)$$

using Eq. (2). The mean excitation energy is found to be  $I = 142$  eV, in good agreement with the value 139.2 eV determined from proton range measurements [19].

Given the model energy-loss function, Eq. (2), differential inverse mean free paths were calculated from Eq. (1). Exchange corrections were included as described previously [13,20]. The inverse mean free path, or the energy loss per unit pathlength, for an electron of energy  $E$  is determined by integrating  $\tau$ , or  $\omega\tau$ , over allowed energy transfers.

### ELECTRON MEAN FREE PATHS

The results for electron inelastic mean free paths are shown in Fig. 3 and listed in Table I with electron energies measured from the bottom of the conduction band. These new results are  $\sim 20\%$  larger than our earlier results [8] for  $E \gtrsim 80$  eV. For comparison, predicted mean free paths for electrons in silicon ( $\rho = 2.33 \text{ g/cm}^3$ ) are also shown where the "dashed" curve is from Ref. 8 and the "dot-dash" curve is from Ref. 21. The difference in these two calculations for silicon is  $\sim 3\%$  for  $E \gtrsim 60$  eV. The curve for Si has approximately the same energy dependence as the curve for  $\text{SiO}_2$  at the higher energies. For very low electron energies, mean free paths in  $\text{SiO}_2$  are much larger than those in Si due to the difference in the band gaps. Experimental data on electron mean free paths in silicon are collected and discussed in the appendix.

Experimental measurements of electron mean free paths from three sources are shown in Fig. 3. The sources of these data are: open circles, Flitsch and Raider [22]; triangles, Klasson et al. [23]; and solid dot, Hill et al. [24]. Reasonably good agreement is found between the theoretical result and the experimental measurements. The data of Flitsch and Raider [22] are consistent with the energy dependence of the model calculation but lie 20-25% below our predicted values. No attempt was made in these comparisons with theoretical inelastic mean free paths to eliminate the contribution of elastic scattering, differences in sample densities, etc.

### STOPPING POWER FOR ELECTRONS

The results for the stopping power of  $\text{SiO}_2$  at a density  $\rho = 2.65 \text{ g/cm}^3$  are shown in Table I in the form  $S' = (1/\rho) (-dE/dx)$  where  $-dE/dx$  is the energy loss per unit pathlength. These values are  $\sim 25\%$  lower than our earlier tabulated results [8] near the Bragg peak around 150 eV but agree to within 1% at 10 keV. For the smaller electron energies, the stopping power is determined entirely by interactions with the valence electrons. As the incident electron energy increases, ionization of the inner shells becomes increasingly important in the stopping process and accounts for  $\sim 30\%$  of the total stopping power at 10 keV.

In Fig. 4 the total stopping power is displayed as a function of electron energy. Also shown is the total inner-shell contribution. For  $E \geq 10 \text{ keV}$  the Bethe-theory calculations of Pages et al. [25], recalculated with  $I = 142 \text{ eV}$ , are given by the dashed curve. The two theoretical calculations differ by  $\sim 1.5\%$  at 10 keV. If the Bethe-theory calculation is extended to lower energies, the difference between the two theoretical predictions increases to  $\sim 5\%$  at 1000 eV. There appear to be no experimental data available for comparison.

### MEAN PATHLENGTHS FOR ELECTRONS

From the stopping power we can determine the mean pathlength traveled by an electron as its energy is reduced from  $E$  to  $E_0$ . This mean pathlength is given by

$$R_{E_0}(E) = \int_{E_0}^E dE' / S'(E'). \quad (5)$$

The results for  $R_{E_0}$  are shown in Fig. 5 for two choices of the "cut-off"

energy  $E_0$  in eV. The shape of the curves at the lower energies is very sensitive to the choice of  $E_0$  since the difference  $R_{10}(E) - R_{20}(E) = \int_{10}^{20} dE' / S'(E')$ , and values of  $S'$  in this energy region are small relative to those near the Bragg peak. The curves become relatively insensitive to  $E_0$  for large  $E$ .

The values of  $R_{10}(E)$  are shown in Table I. The differences in these values may be of more importance than the values themselves. For example, suppose we wanted to know the mean pathlength traveled by an electron of initial energy 300 eV as its energy is reduced to 200 eV. This is given by  $R_{10}(300) - R_{10}(200) = 0.76 \mu\text{g}/\text{cm}^2$  or  $\sim 29\text{\AA}$  for  $\rho = 2.65 \text{ g}/\text{cm}^3$ . For comparison, a 10-keV electron will have a mean pathlength  $\sim 7$  times greater for the same energy loss.

#### DISCUSSION AND CONCLUSIONS

A model for the response of the valence electrons in  $\text{SiO}_2$  to energy and momentum transfers was combined with generalized oscillator strengths for inner-shell ionization to determine a model energy-loss function for  $\text{SiO}_2$ . Various sum rules were employed to constrain and check the overall behavior of this function and insure consistency with known physical properties of the system. From the energy-loss function, differential inverse mean free paths for inelastic processes were derived and used to calculate electron inelastic mean free paths in  $\text{SiO}_2$  and the stopping power of  $\text{SiO}_2$  for electrons. These quantities are useful if one is only interested in the total energy deposited in the medium. However, for studies of the distribution or statistics of the energy deposition processes in the medium, the differential inverse mean free paths are the important



quantities. They form part of the input data for Monte Carlo calculations as described earlier for  $H_2O$  [12,26] and Si [3]. The results of the calculations described in this paper will be incorporated in future studies of the details of energy deposition in thin layers of  $SiO_2$  and can be used in conjunction with Ref. 3 to simulate actual device configurations containing both Si and  $SiO_2$ .

APPENDIX

Electron Mean Free Paths in Silicon

In Fig. 6 we have collected experimental data on mean free paths for comparison with our earlier calculations [7,8] for silicon at a density of  $\rho = 2.33 \text{ g/cm}^3$ . The heavy, solid curve is from Ref. 8. For  $E > 150 \text{ eV}$ , our theoretical result is in good agreement with all the experimental values except those of Klasson et al. [23] indicated by the open triangles. Those values show approximately the same energy dependence as the theoretical predictions but fall some 40-60% higher than the theory curve. The dashed curve is Penn's result [28] for Si assuming silicon is a free-electron-like material; this result agrees quite well with our theoretical predictions (12% lower at  $E = 200 \text{ eV}$ ; 8% lower for  $E > 800 \text{ eV}$ ).

The experimental data (open squares) and theoretical predictions (light, solid curve) of Zaporozhchenko et al. [27] depart significantly from our predictions for  $E < 100 \text{ eV}$ . Their theoretical calculation is based on a quantum field theory approach and may indicate failure of the Born approximation, employed in our calculations [8], at the lower electron energies. This aspect of our calculations deserves further study. However, the difference in energy dependence of their predictions at the higher energies from Penn's [28] or our [8] calculation is somewhat puzzling.

REFERENCES

1. Research sponsored jointly by the Deputy for Electronic Technology, Air Force Systems Command, under Interagency Agreement DOE No. 40-226-70 and the Office of Health and Environmental Research, U. S. Department of Energy, under contract W-7405-eng-26 with the Union Carbide Corporation.
2. On assignment from Computer Sciences Division.
3. R. N. Hamm, J. E. Turner, H. A. Wright, and R. H. Ritchie, *IEEE Trans. Nucl. Sci.* NS-26, 4892 (1979).
4. J. Lindhard, *Kgl. Danske Vid. Sels. Mat. Fys. Medd.* 28(8) (1954).
5. R. H. Ritchie, *Phys. Rev.* 114, 644 (1959).
6. C. J. Tung, R. H. Ritchie, J. C. Ashley, and V. E. Anderson, *Inelastic Interactions of Swift Electrons in Solids*, Oak Ridge National Laboratory Report, ORNL/TM-5188 (1976). Available from NTIS, U. S. Department of Commerce, Springfield, Virginia 22161.
7. J. C. Ashley, C. J. Tung, and R. H. Ritchie, *IEEE Trans. Nucl. Sci.* NS-25, 1566 (1978), and references therein.
8. C. J. Tung, J. C. Ashley, V. E. Anderson, and R. H. Ritchie, "Inverse Mean Free Path, Stopping Power, CSDA Range, and Straggling in Silicon and Silicon Dioxide for Electrons of Energy  $\leq 10$  keV," Air Force Report RADC-TR-76-125 (April 1976). In this tabulation for both Si and SiO<sub>2</sub> the silicon K-shell contribution to inverse mean free paths and stopping powers should be increased by a factor of two. This correction makes only a small change in the total stopping power ( $\sim 1\%$ ) and makes essentially no change in the total inverse mean free path.

9. H. R. Phillip, *Solid State Commun.* 4, 73 (1966).
10. R. B. Laughlin, *Phys. Rev. B* 22, 3021 (1980).
11. G. Klein and H. -U. Chun, *Phys. Status Solidi B* 49, 167 (1972).
12. R. N. Hamm, H. A. Wright, R. H. Ritchie, J. E. Turner, and T. P. Turner, *Proceedings of the Fifth Symposium on Microdosimetry, Verbania, Pallansa, Italy, September 22-26, 1975*, EUR 5452 d-e-f, p. 1037.
13. J. C. Ashley and V. E. Anderson, *J. Electron Spectrosc. Related Phenom.* (to be published).
14. E. J. McGuire, "Calculated Generalized Oscillator Strengths for the Atoms He-Na," Sandia Research Report No. SC-RR-70-406 (May 1971).
15. S. T. Manson (unpublished).
16. E. Merzbacher and H. W. Lewis in *Handbuch der Physik*, edited by S. Flügge (Springer-Verlag, Berlin, 1958), pp. 166-192.
17. U. Buechner, *J. Phys. C: Solid State Phys.* 8, 2781 (1975).
18. U. Fano, *Ann. Rev. Nucl. Sci.* 13, 1 (1963).
19. C. Tschalär and Hans Bichsel, *Phys. Rev.* 175, 476 (1968).
20. J. C. Ashley, C. J. Tung, and R. H. Ritchie, *IEEE Trans. Nucl. Sci.* NS-25, 1566 (1978).
21. J. C. Ashley, C. J. Tung, R. H. Ritchie, and V. E. Anderson, *IEEE Trans. Nucl. Sci.* NS-23, 1833 (1976).
22. R. Flitsch and S. I. Raider, *J. Vac. Sci. Technol.* 12, 305 (1975).
23. M. Klasson, A. Berndtsson, J. Hedman, R. Nilsson, R. Nyholm, and C. Nordling, *J. Electron Spectrosc. Related Phenom.* 3, 427 (1974).
24. J. M. Hill, D. G. Royce, C. S. Fadley, L. F. Wagner, and F. J. Grunthaver, *Chem. Phys. Lett.* 44, 225 (1976).

25. L. Pages, E. Bertel, H. Joffre, and L. Sklavenitis, *Atomic Data* 4, 1 (1972).
26. R. H. Ritchie, R. N. Hamm, J. E. Turner, and H. A. Wright, *Proceedings of the Sixth Symposium on Microdosimetry, Brussels, Belgium, May 22-26, 1978*, EVR 6064 DE-EN-FR, p. 345.
27. V. I. Zaporozhchenko, Yu. D. Kalafati, Yu. A. Kukharenko, and V. M. Sergeev, *Izv. Akad. Nauk SSSR Ser. Fiz.* 43, 1919 (1979).
28. David R. Penn, *J. Electron Spectrosc. Related Phenom.* 9, 29 (1976); *J. Vac. Sci. Technol.* 13, 221 (1976).
29. P. Cadman, G. Gossedge, and J. D. Scott, *J. Electron Spectrosc. Related Phenom.* 13, 1 (1978).

Table I. Electron inelastic mean free paths, stopping powers for electrons, and mean pathlengths of electrons in SiO<sub>2</sub>. The density of SiO<sub>2</sub> is  $\rho = 2.65 \text{ g/cm}^3$ , and electron energies are measured from the bottom of the conduction band.

| E (eV) | $\lambda(\text{\AA})$ | S' (MeV · cm <sup>2</sup> /g) | R <sub>10</sub> ( $\mu\text{g/cm}^2$ ) |
|--------|-----------------------|-------------------------------|--|
| 15     | 170                   | 2.40                          | 4.37                                   |
| 20     | 73.0                  | 6.64                          | 5.64                                   |
| 30     | 23.9                  | 26.2                          | 6.40                                   |
| 40     | 13.7                  | 55.1                          | 6.66                                   |
| 60     | 9.09                  | 105                           | 6.91                                   |
| 80     | 8.40                  | 128                           | 7.08                                   |
| 100    | 8.40                  | 137                           | 7.23                                   |
| 150    | 9.26                  | 141                           | 7.59                                   |
| 200    | 10.4                  | 137                           | 7.95                                   |
| 300    | 12.7                  | 127                           | 8.71                                   |
| 400    | 15.0                  | 117                           | 9.53                                   |
| 600    | 19.5                  | 99.6                          | 11.4                                   |
| 800    | 23.7                  | 87.5                          | 13.5                                   |
| 1,000  | 27.8                  | 78.1                          | 16.0                                   |
| 2,000  | 46.7                  | 52.8                          | 31.9                                   |
| 4,000  | 81.3                  | 33.5                          | 81.0                                   |
| 6,000  | 114                   | 25.1                          | 151                                    |
| 8,000  | 144                   | 20.4                          | 241                                    |
| 10,000 | 173                   | 17.4                          | 348                                    |

FIGURE CAPTIONS

- Fig. 1. The imaginary part of the dielectric function as a function of photon energy. The solid curve is from the optical data of Phillip [9]; the dashed curve is the insulator model fit.
- Fig. 2. The dashed line shows the energy-loss function predicted by the insulator model. The solid curve is from electron energy-loss measurements by Buechner [17].
- Fig. 3. The solid curve is the inelastic mean free path as a function of electron kinetic energy for  $\text{SiO}_2$  at  $\rho = 2.65 \text{ g/cm}^3$ . Also shown for comparison is  $\lambda$  for electrons in Si at  $\rho = 2.33 \text{ g/cm}^3$ ; the dashed curve from Ref. 8 and the dot-dash curve from Ref. 21. Experimental data are from: Ref. 22 -  $\circ$ , Ref. 23 -  $\Delta$ , and Ref. 24 -  $\bullet$ .
- Fig. 4. The stopping power  $S' \equiv (1/\rho)(-dE/dx)$  of  $\text{SiO}_2$  for an electron of kinetic energy  $E$ . The dashed curve is the Bethe-theory result for  $i = 142 \text{ eV}$ .
- Fig. 5. Mean pathlength as a function of electron energy for two values of the "cut-off" energy  $E_0$ .
- Fig. 6. Comparison of theoretical results and experimental data for electron mean free paths in silicon. The heavy, solid curve is from Ref. 8; the light, solid curve from Ref. 27; and the dashed curve from Ref. 28. The sources for the experimental data are:  $\circ$  - Ref. 22;  $\Delta$  - Ref. 23;  $\bullet$  - Ref. 24;  $\square$  - Ref. 27;  $\blacktriangle$  - Ref. 29.

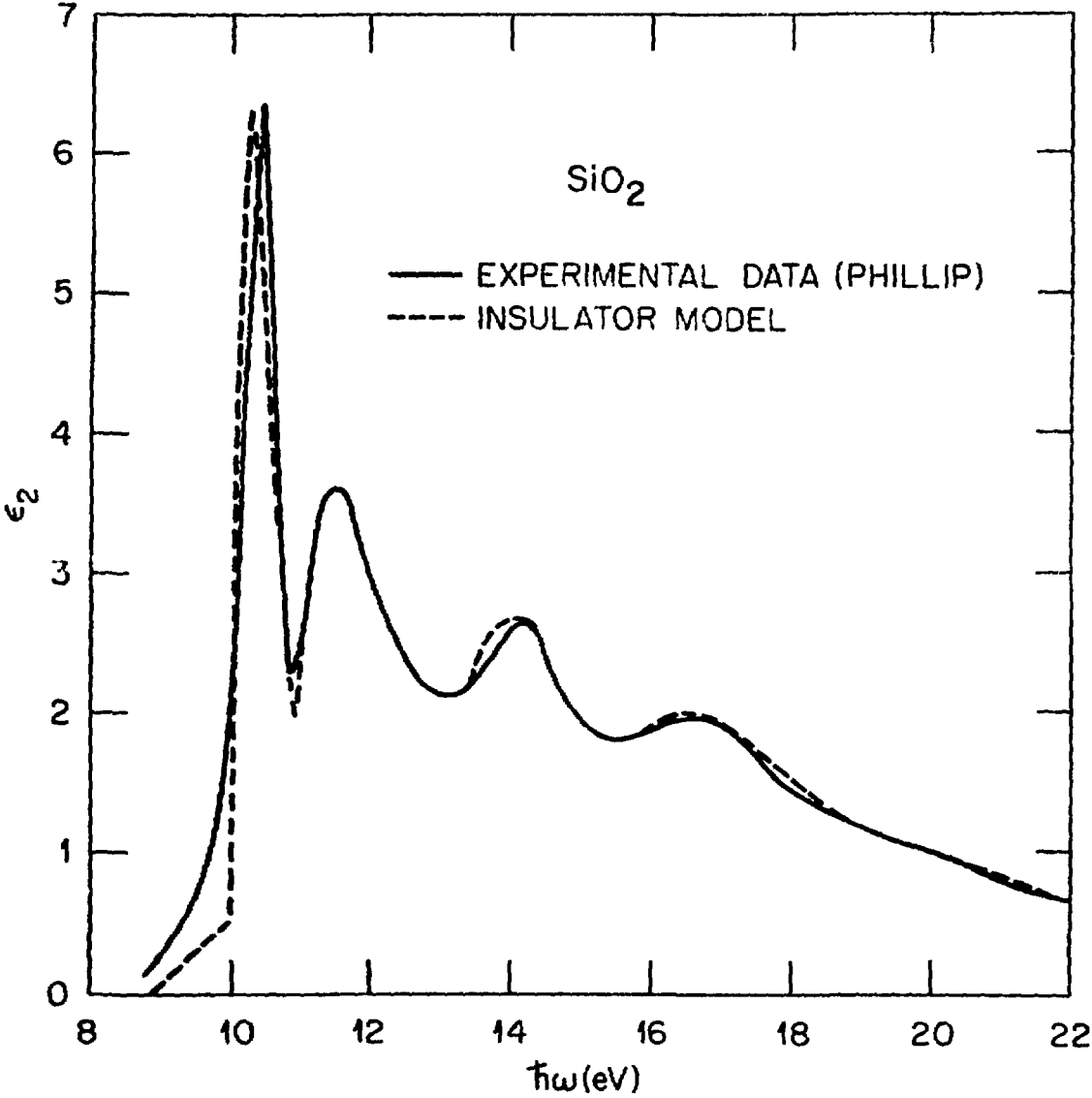


Fig. 1



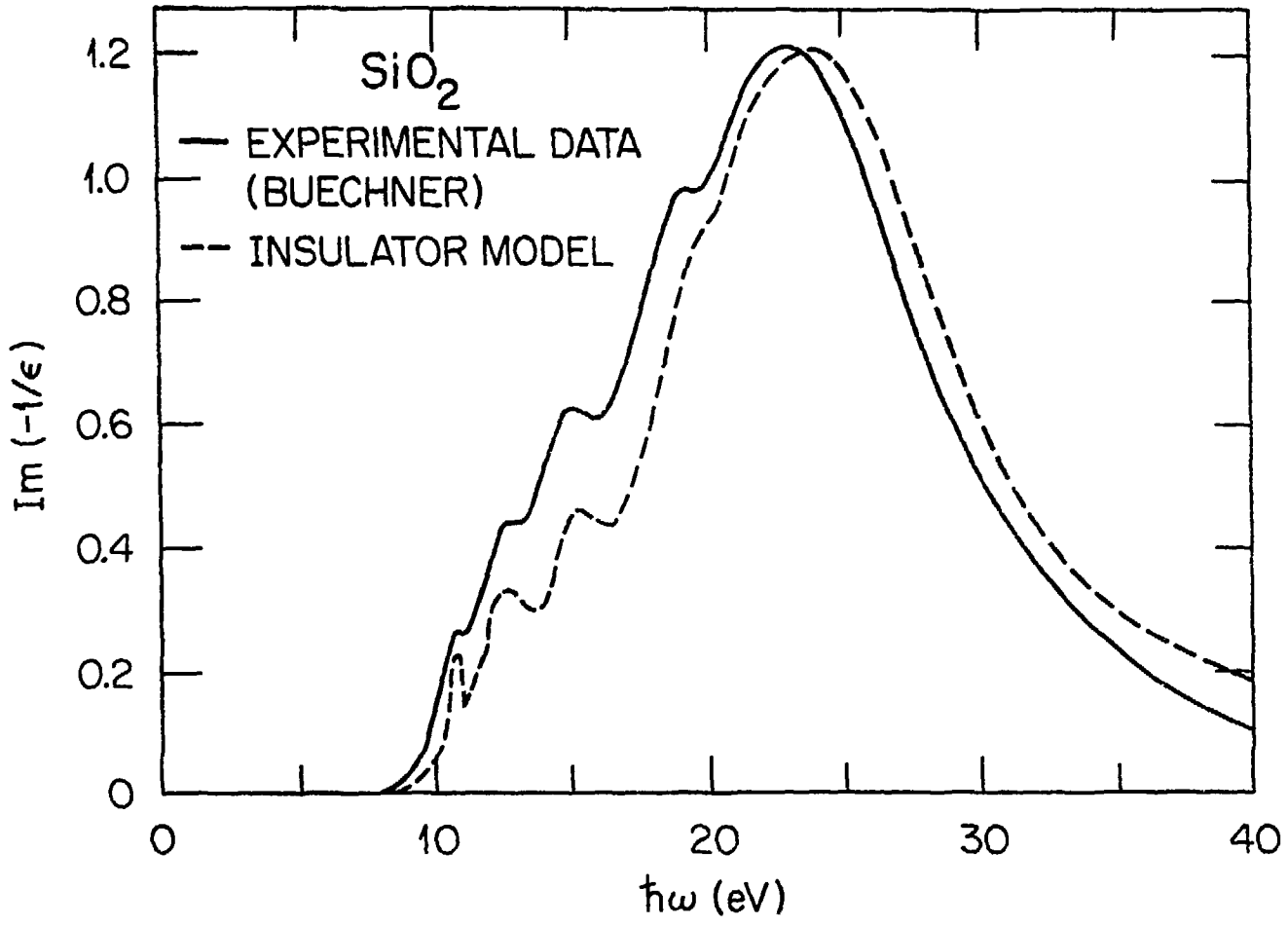


Fig. 2



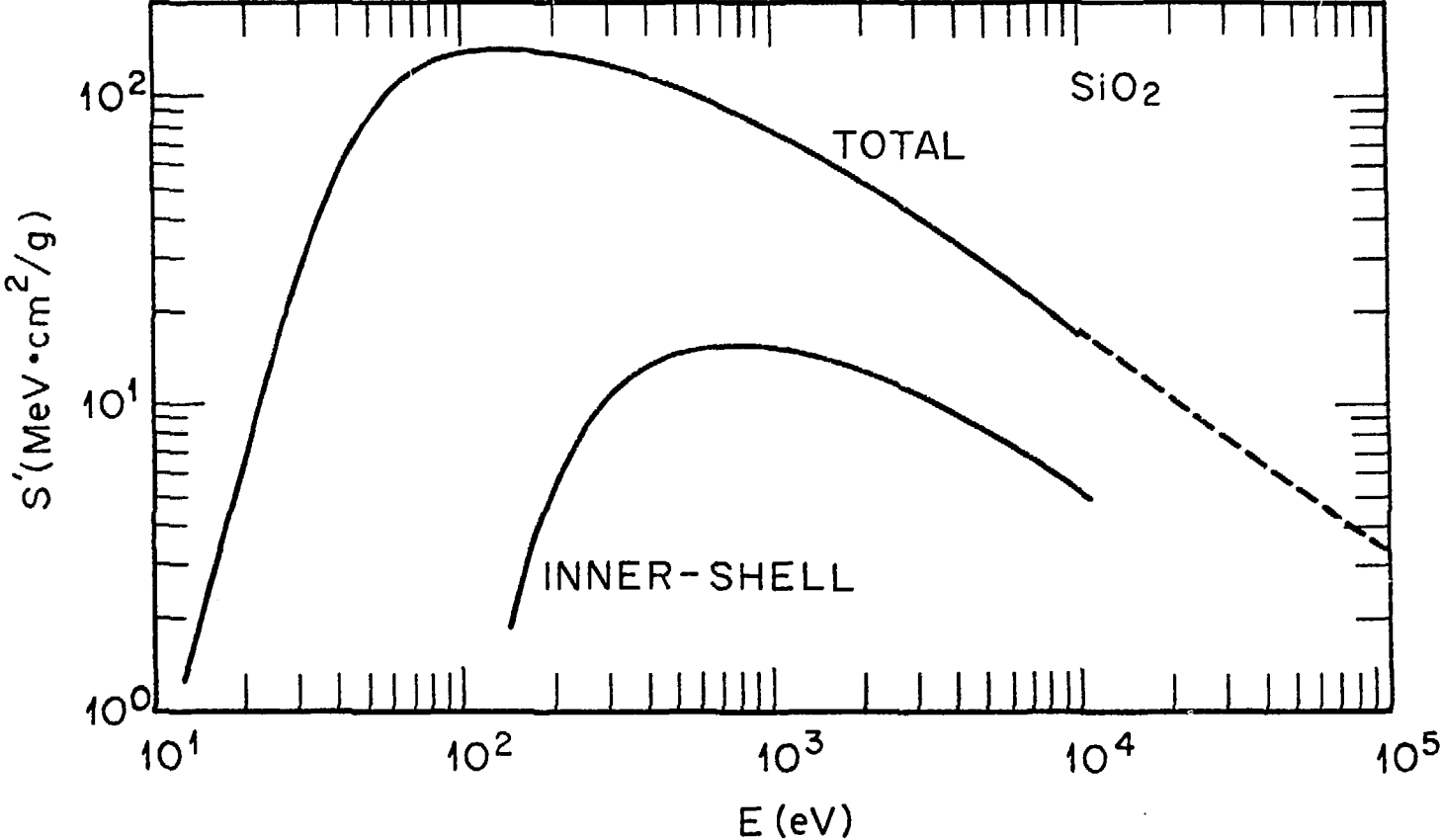


Fig. 4

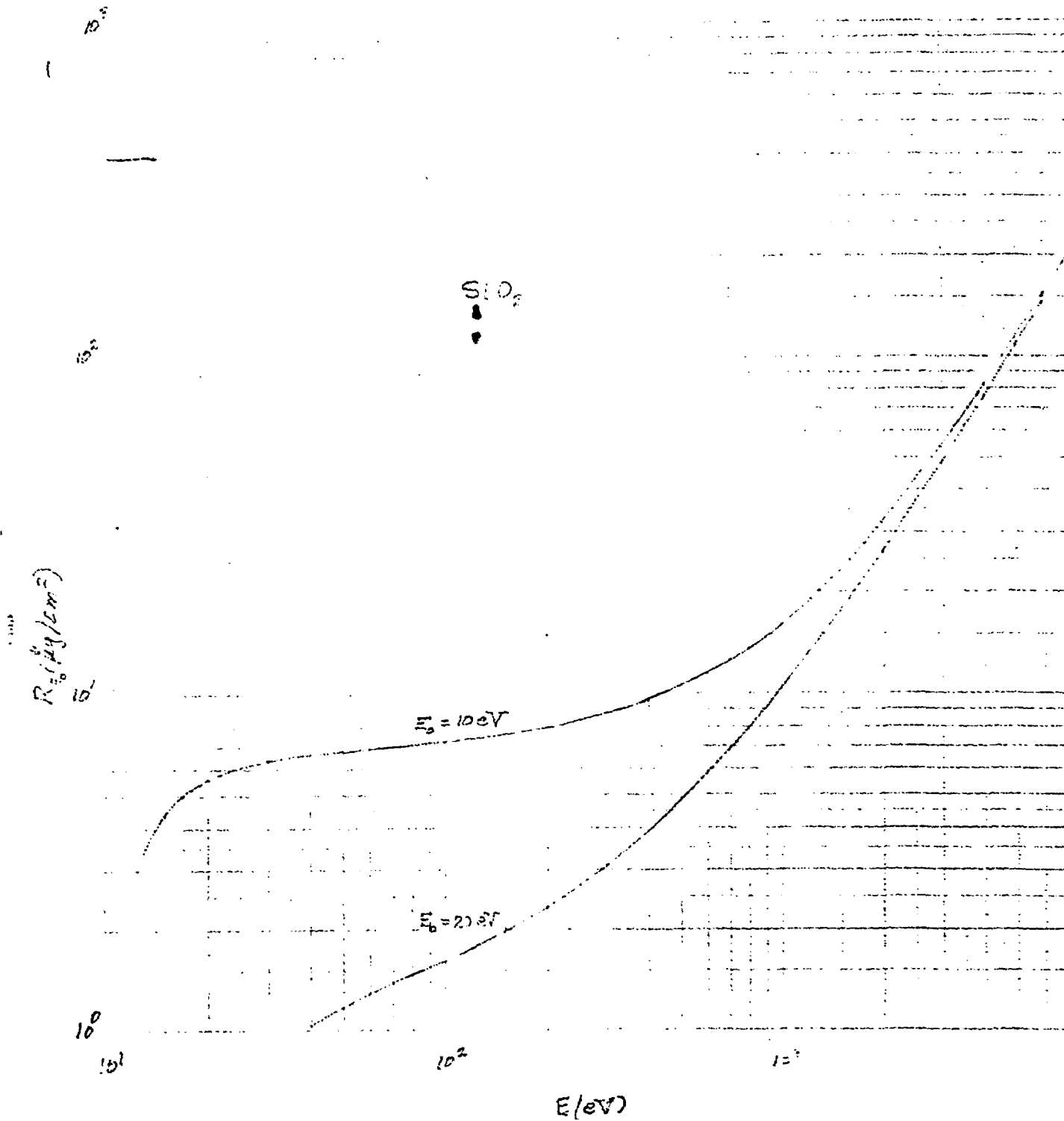


Fig. 5

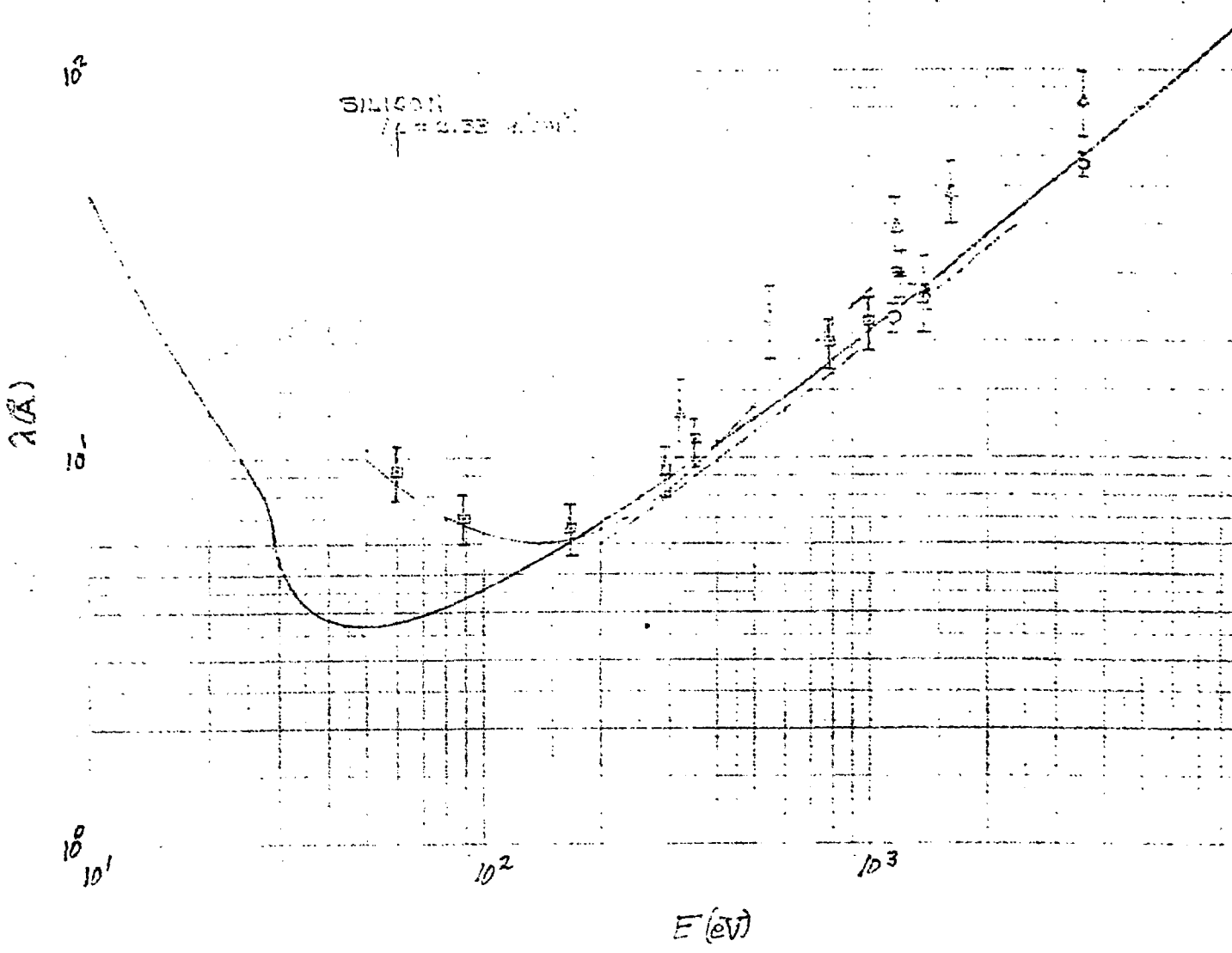


Fig. 6